A MULTI-WAVELENGTH STUDY OF MERCURY'S POLAR ANOMALIES: NEW DATA FROM ARECIBO INFORMED BY MESSENGER

H. Meyer[1], E. G. Rivera-Valentín[2], and N. Chabot[1], [1]Johns Hopkins University Applied Physics Laboratory, Laurel, MD (Heather.Meyer@jhuapl.edu), [2]Lunar and Planetary Institute, USRA, Houston, TX

Introduction: Prior to the arrival of the MESSENGER spacecraft at Mercury, repeat observations of Mercury's polar regions by the Arecibo Observatory (AO) and Goldstone Solar System Radar with the Very Large Array revealed radar-bright features within polar craters consistent with ice deposits [e.g., 1-4 and refs therein]. MESSENGER observations, particularly data from Mercury Laser Altimeter (MLA) and Mercury Dual Imaging System (MDIS), confirmed that these polar anomalies are located in regions of permanent shadow (PSRs) and exhibit surface reflectance values indicative of both exposed surficial ice and lag-deposits of potentially organic-rich volatiles [5-7].

Recent work by [8] further suggests that low-reflectance surfaces associated with PSRs extend beyond the strict limits of the PSRs into dimly lit regions of polar craters, where complex organic compounds can remain stable. A recent campaign by the Arecibo Observatory to improve imaging of Mercury's north polar region provides a new opportunity to assess the distribution of volatiles at Mercury informed by the wealth of new knowledge resulting from the MESSENGER mission. This work builds on the analyses by Rivera-Valentín et al. (2021) [9], who used machine learning algorithms to identify small scale variations in radar backscatter. Their work demonstrated that the north polar anomalies are not homogeneous and that differences, perhaps due to burial depth and relative ice abundance, can be discerned from S-band radar observations over several days [9]. Here, informed by MDIS and MLA data, we continue their k-means clustering analysis to assess the finer-scale variations observed in S-band backscatter data, validate the machine learning method against geologic observations, and further characterize Mercury's polar ice deposits.

Data and Methods: We use new Arecibo S-band (12.6 cm; 2380 MHz) radar observations of Mercury taken during the 2019 and 2020 inferior conjunctions, the first taken of Mercury's north pole since MESSENGER visited Mercury. As detailed in [9], we used the long-code delay-Doppler radar imaging method [10] to produce delay-Doppler images of Mercury in both the opposite circular (OC) and same circular (SC) polarization as transmitted. Radar images were then transformed to hermiocentric coordinates and projected into a polar stereographic map using standard techniques [11-12]. To assess local-scale variations in the radar-scattering properties of the individual deposits, we employed an unsupervised *k*-means clustering algorithm

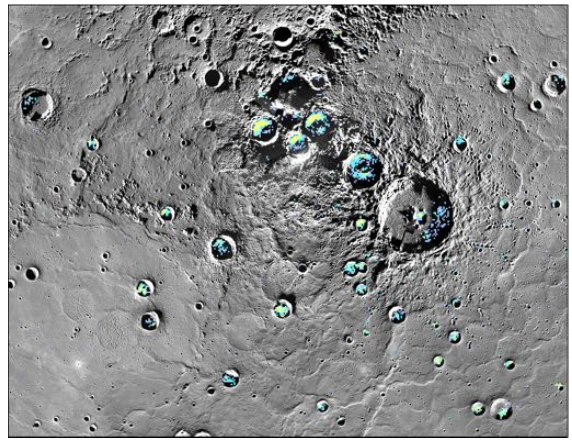

Figure 1: A 2 km/pixel *k*-means map for the north polar region of Mercury of S-band radar SC backscatter from [9]. Yellow indicates the highest *k*-means class, denoting the strongest backscatter signal, with green and blue denoting the next two classes below, respectively.

using the CH index [13]. This technique clusters data into groups that are then represented by their cluster mean and standard deviation. This allows for a direct and robust pixel-by-pixel comparison of radar backscatter across polar deposits. Although the radar imaging would at best allow for a resolution of 750 m/pixel, in order to increase the SNR for our analysis, the base radar image used for the *k*-means clustering is 2 km/pixel.

In [9], the *k*-means clustering algorithm was used over the entire radar image to identify signal that was robustly distinguishable from noise and to study its spatial variation. Here, we further the technique by clustering only those data points that are robustly distinguishable from noise, i.e., by taking the signal from the top two *k*-means classes from [9] and applying the same clustering analysis to only that signal. This allows us to study the small-scale local variation in radar backscattering within the polar deposits and discern finer details within the areas of strongest SC backscatter. The *k*-means maps were then compared to the radar observations by Harmon et al. (2011) [4] and to the local geology using MLA 1064-nm reflectance measurements [5] and MDIS mosaics [14], with particular attention to craters that exhibit anomalous MLA reflectance [5].

Analysis: Overall, locations identified by *k*-means clustering as robust signal for a given day is consistent with earlier radar observations [3] (Fig. 1). The cluster maps over the SC backscatter radar images summed over the six-day observing runs show more extensive

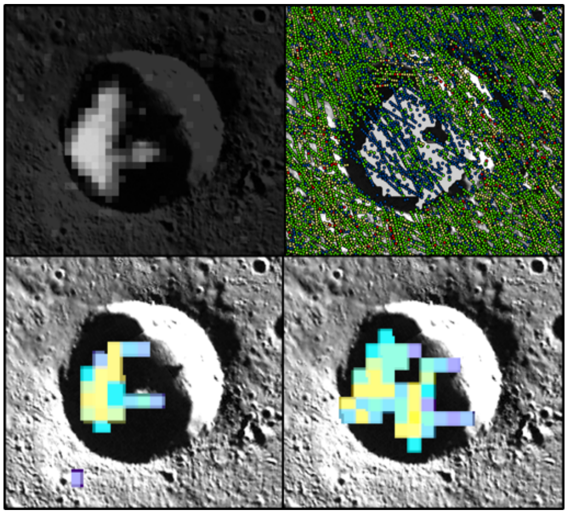

Figure 2: Laxness crater (∼26 km in diameter) (top left) pre-MESSENGER AO S-band backscatter [3], (top right) MLA 1064 nm reflectance (red≥0.3, yellow=0.2-0.3, green=0.1-0.2, and blue≤0.1 after [15]) overlain on an MDIS mosaic with the extent of the PSR shown in white, (bottom left) the *k*-means map for the July 19, 2019 SC backscatter observation from AO, (bottom right) and the *k*-means map for the SC backscatter radar image summed over the entire 2019 observing run. *k*-means classes identical to Fig. 1.

radar bright signatures than previous work (see bottom right panel of Fig. 2). The areas of strongest SC backscatter (yellow class) are co-located with the innermost sections of PSRs as defined by [15]. Lower classes (i.e., greens and blues) are associated with crater walls, central peaks, and the edges of the PSRs. These areas receive more secondary illumination, so the lower classes are consistent with the interpretation that ice is less stable in these areas. This is consistent with the overall interpretation from [9]. Here, finer-scale variations are more immediately identifiable and closely align to the margins of PSRs.

In the case of Laxness crater (Fig. 2), previous observations indicated that Laxness exhibits low MLA reflectance (top right), but is radar bright [3] (top left). Our *k*-means analysis demonstrates that while the PSR in Laxness remains radar bright as of 2019 (bottom left and right), it exhibits variations consistent with the variation in secondary illumination. The yellow (strongest) class is observed in the innermost part of the PSR. Of note, the blue class in particular corresponds not only to the margin of the PSR and nearby slopes, but also to the edge of the low reflectance zone observed in MLA. This confirms previous interpretations that the ice present in the Laxness PSR is buried beneath a thin, low reflectance overburden. Given that the area is radar-bright in S-band, the deposit should be within the upper ∼1 m of the surface.

On the other hand, the Prokofiev PSR exhibits overall lower *k*-means classes and sparse robust signal in its floor, despite the high reflectance observed by MLA. This association of radar bright deposits with high reflectance is only observed for a few very small locations within PSRs that also exhibit high (yellow or green) *k*-means classes and none with reflectance values as high as at Prokofiev. The preponderance of lower classes within Prokofiev may indicate a lower abundance of near-surface ice, potentially a thin surficial layer. When considered in conjunction with MLA observations, it may also indicate that the PSR has been gardened sufficiently to expose ice at the surface and to remove the bulk of the subsurface ice from this PSR. Alternatively, if the Prokofiev PSR never trapped the same quantity of volatiles observed within its neighbors (including two small craters in the Prokofiev floor and one small crater just outside Prokofiev), then it may be possible to use the differences in SC backscatter to put constraints on the timing and/or origins of the polar volatiles.

Conclusions: We used new S-band Arecibo planetary radar observations along with machine learning algorithms to discern fine-scale features within Mercury's polar deposits. In tandem with MESSENGER MLA and MDIS data, our analysis indicates that local-scale variations may be associated with higher concentrations of ice both across individual deposits due to local environmental factors and relative to other polar PSRs. Additionally, our analysis supports previous work suggesting that deposits such as Laxness, which exhibit anomalously low MLA 1064 nm reflectance, still retain high concentrations of ice in the upper meter of the surface.

Acknowledgements: This research was supported by NASA through DDAP under Grant No. 80NSSC19K0881, NEOO under Grant No. NNX13AQ46G, and SSO under Grant No. 80NSSC19K0523.

References: [1] Slade, M. A. et al. (1992) Science 258, 635-640. [2] Harmon, J. K. & Slade, M. A. (1992) Science, 258, 640-643. [3] Butler, B.J. et al. (1993) JGR 98, 15003–21. [4] Harmon, J. K. et al. (2011) Icarus 211, 37-50. [5] Neumann et al., (2013) Science 339, 296-300. [6] Chabot et al., (2014) Geology 42(12), 1051–1054. [7] Chabot et al. (2016) Geophys. Res. Lett. 43, doi:10.1002/ 2016GL070403. [8] Hamill et al. (2020) Planet. Sci. J. 1(3), 57. [9] Rivera-Valentín et al. (2021) this meeting. [10] Harmon, J. K. (2002) IEEE Trans. G&RS 40, 1904-1916. [11] Pettengill, G. H. et al. (1974) The Moon, 10, 3-16. [12] Campbell, B. A. (2002) Cambridge Univ. Press. [13] Calinksi, T. & Harabasz, J. (1974) Comm. in Stats. 2, 1-27. [14] Denevi et al. (2018), Space Sci. Rev. 214, 2. [15] Deutsch, A. N. et al. (2016) Icarus 280, 158-171.